Science of the Total Environment 658 (2019) 669–683

Contents lists available at ScienceDirect

Science of the Total Environment

journal homepage: www.elsevier.com/locate/scitotenv

Monitoring land sensitivity to desertification in Central Asia: Convergence or divergence?

Liangliang Jiang [a,b,c,d,e], Anming Bao [a,d,e,*], Guli Jiapaer [a,d,e], Hao Guo [a,b,c,d,e], Guoxiong Zheng [a,b], Khusen Gafforov [a,b,f], Alishir Kurban [a,d,e], Philippe De Maeyer [c,d,e]

[a] State Key Laboratory of Desert and Oasis Ecology, Xinjiang Institute of Ecology and Geography, Chinese Academy of Sciences, Urumqi 830011, China
[b] University of Chinese Academy of Sciences, Beijing 100049, China
[c] Department of Geography, Ghent University, Ghent 9000, Belgium
[d] Sino-Belgian Joint Laboratory of Geo-information, Urumqi 830011, China
[e] Sino-Belgian Joint Laboratory of Geo-information, Ghent 9000, Belgium
[f] Research Institute of Irrigation and Water Problems, Tashkent 100187, Uzbekistan

HIGHLIGHTS

- Spatial convergence patterns were a relevant predictor of desertification risk.
- Divergence patterns from 1992 to 2000 in the northern region resulted from human activities.
- Convergence patterns from 2000 to 2015 in most areas were caused by climate change.
- Low sensitivity area trends converged under precipitation change.

GRAPHICAL ABSTRACT

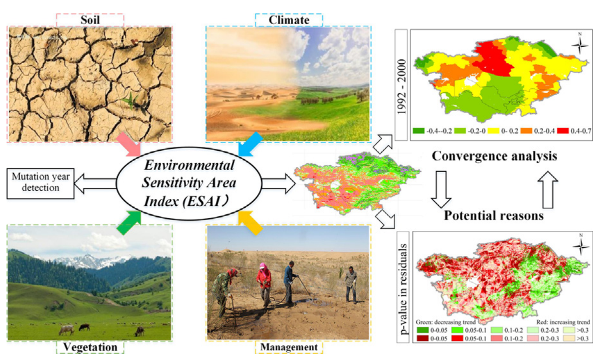

ARTICLE INFO

Article history:
Received 26 September 2018
Received in revised form 8 December 2018
Accepted 10 December 2018
Available online 12 December 2018

Editor: Ashantha Goonetilleke

Keywords:
Desertification risk
Environmental sensitivity area index
Convergence analysis
Climate change
Human activities

ABSTRACT

In Central Asia, desertification risk is one of the main environmental and socioeconomic issues; thus, monitoring land sensitivity to desertification is an extremely urgent issue. In this study, the combination of convergence patterns and desertification risk is advanced from a technical perspective. Furthermore, the environmentally sensitive area index (ESAI) method was first utilized to monitor the risk of desertification in Central Asia. In the study, the spatial and temporal patterns of desertification risk were illustrated from 1992 to 2015 using fourteen indicators, including vegetation, climate, soil and land management quality. The ESAI spatial convergence across administrative subdivisions was explored for three time intervals: 1992–2000, 2000–2008 and 2008–2015. The results indicated that nearly 13.66% of the study area fell into the critical risk of desertification from 1992 to 2008. However, the risk of desertification has improved since 2008, with critical classifications decreasing by 19.70% in 2015. According to the mutation year detection in the ESAI, 25.89% of the pixels with mutation years from 1992 to 2000 were identified, and this value was higher than that during the other time periods. The convergence analysis revealed that the desertification risk for 1992–2000 tended to diverge with a positive convergence coefficient of 0.13 and converge over the 2000–2008 and 2008–2015 time periods with negative convergence coefficients of −0.534 and −0.268, respectively. According to the spatial convergence analysis, we found that the divergence patterns in northern Central Asia from 1992 to 2000 resulted from the effects of the Soviet Union collapse: cropland abandonment in northern Kazakhstan and rangeland abandonment in

* Corresponding author at: State Key Laboratory of Desert and Oasis Ecology, Xinjiang Institute of Ecology and Geography, Chinese Academy of Sciences, Urumqi 830011, China.
E-mail address: baoam@ms.xjb.ac.cn (A. Bao).

https://doi.org/10.1016/j.scitotenv.2018.12.152

Tajikistan, Kyrgyzstan and eastern Kazakhstan. In contrast, most areas from 2000 to 2008 experienced increased sensitivity to desertification with the convergence pattern caused by decreased precipitation, especially in northern Central Asia. However, convergence patterns were found in most regions for 2008–2015 with regard to augmented precipitation, which resulted in decreased sensitivity to desertification. Moreover, the low sensitivity areas were more likely to converge under increased precipitation. In this region, the findings of our study suggested that spatial convergence and divergence acted as related predictors of climate change and human activities, respectively. Thus, the ESAI convergence analysis was considered to provide an early warning of potential desertification.

1. Introduction

Currently, desertification is considered one of the major environmental issues in the world. Desertification currently affects over one-third of the world's land and aggravates and contributes to socioeconomic and environmental issues, such as a lack of food security, poverty and the reduction or loss of biodiversity (UNCCD, 2017). Desertification remains widespread and poses serious challenges for sustainable development, particularly in arid and semiarid zones (Fleskens and Stringer, 2014). The arid zone contains >1 billion people who are living in poor conditions and are threatened by desertification (Assessment ME, 2005), and most of these people live in vulnerable areas and may be severely affected by desertification. Moreover, Central Asia includes three temperate deserts, the Karakum, Kyzylkum and Muyunkum Deserts, and contains one of the world's largest arid zones (Fig. 1). This arid area across Northern Eurasia is a dryland hotspot dominated by a fragile ecological environment (Loboda et al., 2012). Due to the relative transformation of the socioeconomic development models before and after the collapse of the Soviet Union, the ecological environment in Central Asia was very sensitive during that time (Behnke and Mortimore, 2016; Seddon et al., 2016). This area underwent the Aral Sea disaster and soil salinization (Kienzler et al., 2012). However, the recent sensitivity of this region to desertification is not well understood.

The definition of desertification from the United Nations Convention to Combat Desertification (UNCCD) is widely used and accepted (London NSFSD and Unep N, 1994). Based on this definition, desertification can be caused by climatic variations and human activities. Anthropogenic activities and climate change in Central Asia have demonstrated obvious regional characteristics over recent decades. Central Asia experienced land reclamation during the Soviet Union and the abandonment of extensive cultivated fields since the collapse of the Soviet Union, which has greatly affected the desertification risk (Lioubimtseva and Henebry, 2009; Propastin, 2008). Another significant impact on desertification sensitivity was the collapse of animal husbandry since 1990, which resulted in the abandonment of distant pastures (Klein et al., 2012; Xi and Sokolik, 2016). Additionally, the temperature (affected by global warming in Central Asia) has been rapidly rising, since the mid-1990s, the temperature has been higher than at any other time in history (Davi et al., 2015; Li et al., 2015). Precipitation has presented spatially heterogeneous changes and a slight decrease (Li et al., 2015; Mannig et al., 2013). In this area, ecosystems with low biodiversity have been susceptible to fluctuations in desertification sensitivity under high climatic fluctuations and anthropogenic activities over the last several decades (Han et al., 2016; Zhou et al., 2015b), especially in the three temperate deserts (Fig. 1) (Zhang et al., 2016). Furthermore, the desertification problem has been an important

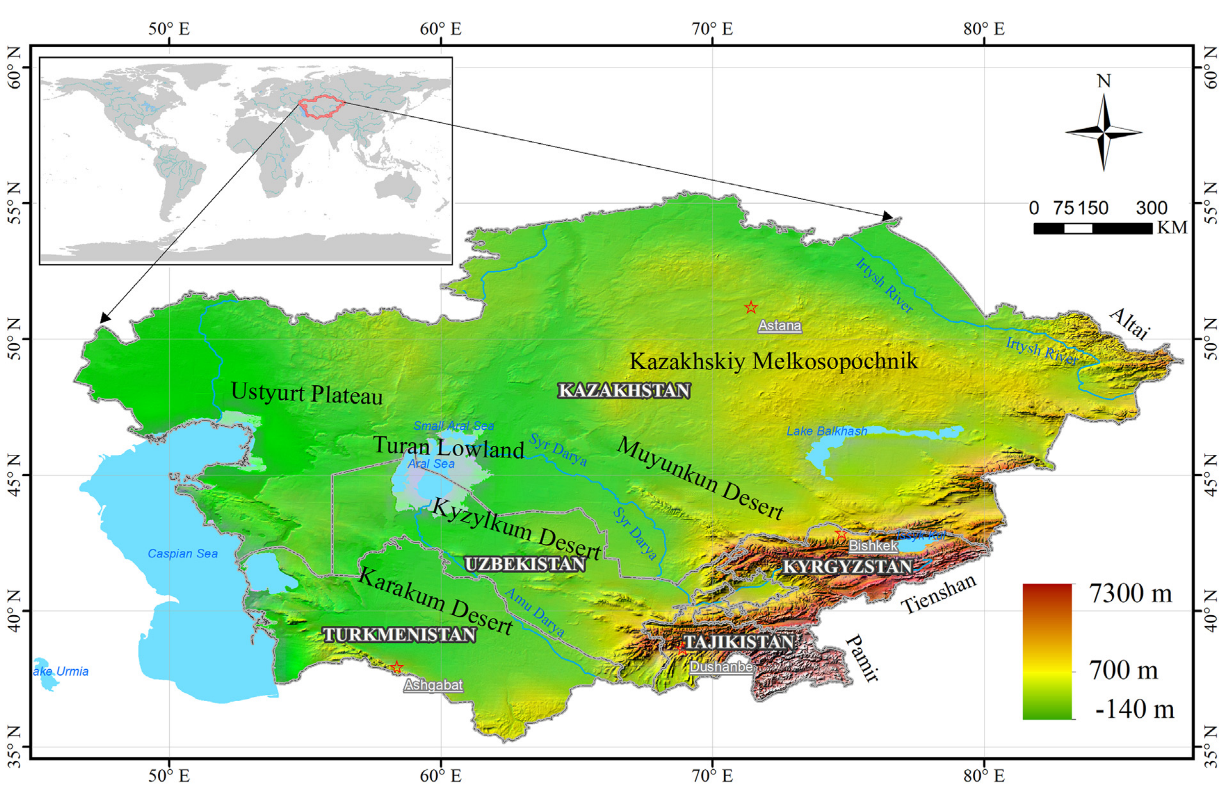

Fig. 1. Topographic map of the five Central Asian countries. National boundaries were downloaded from the National Administration of Surveying, Mapping and Geoinformation, No. GS (2016) 1665.

concern for ecosystem services and human well-being (D'Odorico et al., 2013; Wang et al., 2017). Thus, desertification risk has attracted increasing attention in Central Asia along with climate change and human activities as global research hotspots. However, the different driving factors of desertification have received little consideration in this region.

Different methodologies have been applied to monitor desertification risk on a regional and global scale based on the related indicators (Becerril-Piña et al., 2015; Kundu and Dutta, 2011; Vorovencii, 2017; Wang et al., 2017; Zhou et al., 2015a). Most studies select only one or two indicators, such as albedo and the normalized difference vegetation index (NDVI), either separately or jointly, to monitor desertification risk (Kundu and Dutta, 2011; Li et al., 2016; Ma et al., 2011). The proposed indicators in previous studies can promote the development of desertification risk assessments based on remote sensing and GIS technology. The lack of standardized methodology results in various desertification risk assessments. Although desertification risk is closely related to vegetation, the main desertification features are also related to drought and soil conditions according to the strategic indicators of the UNCCD (Sommer et al., 2011). The production of (desertification risk) indexes using a comprehensive assessment to select several indicators for desertification risk monitoring would be a reasonable aim. Unfortunately, long time series and large-scale studies have been neglected because of limited dataset availability (Salvati, 2012). Previous studies selected several period datasets to assess desertification and did not consider the desertification process peculiarities in time series datasets (Lamchin et al., 2016; Pan and Li, 2013). Hence, it is crucial that time series datasets from 1992 to 2015 be considered in our study. The desertification risk used in this context was defined by Kosmas et al. (Kosmas et al., 2013), and it has been widely accepted as “the vulnerability or sensitivity of the land to further degradation and desertification according to existing soil, vegetation, climate, and management characteristics” (Prăvălie et al., 2017b; Salvati et al., 2016). The environmentally sensitive area index (ESAI) methodology incorporates soil, vegetation, climate and management quality and is one of the most widely used approaches for monitoring desertification risk (Kosmas et al., 1999), which views the desertification process based on the proposed classification scheme and indicator scores from a multidisciplinary standpoint. Many indicators of each quality can be chosen to solve the dataset limitations. This approach was first designed for the European continent and later applied worldwide, including in arid and semiarid regions (Bakr et al., 2012; Contador et al., 2009; Farajzadeh and Egbal, 2007; Hooke et al., 2005). The aim in this study is to design a composite index called the ESAI for monitoring land sensitivity. It is extremely urgent to monitor desertification risk in Central Asia because of the high levels of climate change and human activities.

The “convergence” notion was generalized from the economic concept of “conditional convergence”, which is commonly applied to the indicators of an economy's growth rate or the economy's level of income (Barro and Sala-I-Martin, 2004). According to this concept, adjacent areas tend to converge to the same stable state. Thus, the convergence analysis can test systems that have similar spatial characteristics. Regional disparities among different policies regarding divergence can be observed in environmental processes. To date, convergence assessments have been widely applied on regional and national scales considering economic and social indicators (Giannias et al., 1999; Manca et al., 2014), although few environmental quality studies have been conducted considering spatial convergence (Ezcurra, 2007; Tombolini et al., 2016). Thus, studies of spatial convergence considering ecological indicators are needed as potential evidence to alleviate desertification processes driven by climatic variations and anthropogenic activities, jointly or separately (Tombolini et al., 2016). The convergence notion was first applied to desertification sensitivity in Italy (Salvati and Zitti, 2008). Spatial convergence or divergence can be regarded as a possible indicator of desertification in a complex environment (Salvati, 2014; Tombolini et al., 2016). In the context of climatic variations and human pressure on fragile ecosystems, understanding desertification risk by spatial convergence is necessary to develop socioenvironmental scenarios for policy implementation in ecological environments of Central Asia (Zhang et al., 2017).

To meeting these requirements, the ESAI and spatial convergence methodologies were first utilized for monitoring desertification risk to fill this research gap, which appears to be meaningful in Central Asia. The soil, climate, vegetation and land management quality domains include fourteen indicators that were chosen using the ESAI methodology. The aim of this study is to (1) monitor the spatial and temporal patterns of the quality indicators and ESAI; (2) analyse spatial convergence in the ESAI in time intervals on the spatial scale of administrative subdivisions; and (3) detect the relative roles of climate change and human activities on desertification risk. Finally, the potential reasons for the ESAI convergence and divergence patterns were discussed. By understanding the spatial and temporal characteristics of desertification risk, we aim to contribute to the protection of the ecological environment and to maintain the ecosystem services in this region.

2. Materials and methods

2.1. Study area

The study area comprises five states of the Commonwealth of Independent States (CIS): Kazakhstan, Uzbekistan, Kyrgyzstan, Tajikistan and Turkmenistan, which are collectively known as Central Asia (Fig. 1) (Bohovic, 2016; Gessner et al., 2013). Central Asia spans from the Caspian Sea in the west to China in the east and from Russia in the north to Iran, Afghanistan and Pakistan in the south, covering an area of approximately 4 million km^2. The region is subdivided into 444 administrative subdivisions of five countries that were considered elementary spatial units for the convergence analysis.

The altitude gradually decreases from the Altai, Tien Shan and Pamir Mountains to the western coast of the Caspian Sea (de Beurs et al., 2015). Central Asia is located in a temperate continental climate zone characterized by strong spatial and seasonal differences in rainfall and temperature, with hot-dry summers in the plains and cold-moist winters in the mountains (Xu et al., 2016). The annual precipitation varies from <100 mm in the plain zones to >600 mm in the mountain zones (Klein et al., 2012). The annual temperature changes from <0 °C in the mountain zones to >18 °C in the southern desert zones (Mohammat et al., 2013). The potential evapotranspiration in Central Asia experienced an overall increased trend in recent decades. Notably, the significantly increased trends were especially concentrated in western Kazakhstan and the Aral Sea region, with annual change rates of up to 7.42 mm/a (Fig. S1, Supplementary material). According to the difference between precipitation and potential evapotranspiration, most areas were subjected to a negative climatic water balance, especially in western Kazakhstan and the Aral Sea region (Guo et al., 2018a; Guo et al., 2018b).

The ecological environment in Central Asia is vulnerable to desertification issues related to salinization, overexploitation of arable land, agricultural abandonment, overgrazing, drought and so on (Jiang et al., 2017; Kraemer et al., 2015; Saiko and Zonn, 2000). Central Asia contains 80% of the global temperate deserts, which represent fragile ecological environments in most regions (Kottek et al., 2006). The main land use types include croplands, grasslands, shrublands and sparse vegetation, which account for 22.04%, 25.84%, 6.83% and 39.97% of the study area, respectively (Fig. S1, Supplementary material). The southern plain region is dominated by sparse vegetation because three temperate deserts are located in this area. The Amu Darya and Syr Darya are well known for large-scale irrigated agriculture (de Beurs et al., 2015). Furthermore, after the disintegration of the Soviet Union, the region's socioeconomic conditions experienced varying degrees of change, leading to increased desertification risk. Therefore, it is extremely urgent to monitor the land sensitivity to desertification in this area.

2.2. Data and indicators

The ESAI approach is broadly applied for monitoring desertification risk on a regional scale (Bakr et al., 2012; Prăvălie et al., 2017a; Prăvălie et al., 2017b; Salvati et al., 2016; Zambon et al., 2017). The ESAI approach was pioneered by the Department for Environment, Food and Rural Affairs of the UK in 1987 and was improved by Kosmas (Kosmas et al., 1999). Combined with field investigations, the key indicators proposed by Kosmas have been identified for assessing desertification risk in the MEDALUS (Mediterranean desertification and land use) project based on the correlation between the variable and land degradation. Based on the ESAI framework (Fig. S2, Supplementary material), fourteen indicators were chosen to consider four quality domains: vegetation, climate, soil and land management (Table 1). Each quality index was calculated from several indicator parameters. The value of each parameter was categorized into several classes, the thresholds of which were determined according to extensive field work during the MEDALUS project. Then, sensitivity scores between 1 (lowest sensitivity) and 2 (highest sensitivity) were assigned to each class based on the importance of the class' role in land sensitivity to desertification and the relationships of each class to the onset of the desertification process or irreversible degradation. A more comprehensive description of how the indicators are related to desertification risk and scores is provided in the studies of Kosmas (Kosmas et al., 2013; Kosmas et al., 1999).

2.2.1. Soil quality index

The soil quality index (SQI) can influence the soil state because the resistance to water storage and erosion and can reflect the ability of

Table 1
Classes and scores of indicators used for calculating the soil, climate, vegetation and management qualities.

Domain	Indicator	Class	Characteristic	Score	Role of each indicator
SQI	Texture	1	Clay (heavy), Silty clay, Clay (light), Silty clay loam	1	Different soil textures react differently to soil erosion, vegetation and desertification. Sand and Sandy loam are liable to desertification.
		2	Clay loam, Silt, Silt loam	1.2	
		3	Sandy clay, Loam, Sandy clay loam	1.6	
		4	Sand, Loamy sand, Sandy loam	2	
	Soil salinity	1	Null, None or slight, Mainly non-soil, Permafrost area, Water bodies	1	Increasing salts content results in a potentially adverse ecological environment for croplands or natural vegetation, leading to desertification.
		2	Moderate	1.4	
		3	Severe	1.7	
		4	Very severe	2	
	Drainage	1	Well, Moderately well	1	Absent drainage leads to salt accumulation, resulting in desertification.
		2	Imperfectly, Somewhat excessive	1.2	
		3	Poor, Excessive, Very poor	2	
	Topsoil clay fraction (%)	1	>25	1	Soil moisture conservation, biomass production and soil erosion are affected.
		2	10–25	1.3	
		3	<10	2	
	Slope (%)	1	<6	1	Topography is an important determinant of soil erosion.
		2	6–18	1.2	
		3	18–35	1.5	
		4	>35	2	
CQI	Rainfall (mm)	1	>650	1	Distribution of rainfall distribution is the major determinants of biomass production.
		2	280–650	1.5	
		3	<280	2	
	Aridity	1	>0	1	Aridity is a critical environmental factor for natural vegetation, which may lead to reducing vegetation cover under the water stress.
		2	−0.8-0	1.2	
		3	−0.8–1.6	1.4	
		4	−2.4–1.6	1.8	
		5	<−2.4	2	
	Aspect	1	NW − NE	1	Aspect affects the desertification process through the microclimate by regulating isolation.
		2	SW − SE	2	
VQI	Fire risk	1	Bare land, Perennial agricultural crop, Annual agricultural crop	1	Fire risk causes land degradation and biodiversity losses.
		2	Evergreen forest, Mixed forest	1.3	
		3	Shrub, Grassland	1.6	
		4	Evergreen forest	2	
	Erosion protection	1	Broadleaved forest, Mixed forest	1	Erosion protection decreases land sensitivity to desertification.
		2	Shrub, Grassland,	1.3	
		3	Deciduous forest	1.6	
		4	Perennial agricultural crop	1.8	
		5	Annual agricultural crop, Bare land	2	
	Drought resistance	1	Mixed forest, Evergreen forest	1	Droughts cause a reduction in leaf area index and increase soil erosion.
		2	Deciduous forest	1.2	
		3	Perennial agricultural tree	1.4	
		4	Perennial grassland, Shrub	1.7	
		5	Annual agricultural crop, Annual grasslands, bare land	2	
	Plant cover (%)	1	>40	1	Reduction in plant cover is considered to be an indicator of the onset of desertification.
		2	10–40	1.8	
		3	<10	2	
MQI	Agricultural intensity	1	Natural vegetation, forest, beaches, dunes, sands	1	Intensive cultivation results in accelerated erosion and land degradation.
		2	Rainfed cropland, cropland with natural vegetation	1.5	
		3	Permanently irrigated land	2	
	Policy enforcement	1	Permanently irrigated land, broadleaved forest	1	Policy enforcement is related to land protection for combating desertification.
		2	Cropland with natural vegetation	1.5	
		3	Rainfed cropland, natural vegetation, forest, beaches, dunes, sands	2	

Classification scheme, indicator scores and role of each indicator were adopted based on the ESAI approach in the work of Kosmas (Kosmas et al., 1999). A more comprehensive description of the role of each indicator related to desertification risk is provided in the studies of Kosmas (Kosmas et al., 2013; Kosmas et al., 1999).

soil to sustain natural vegetation (Salvati and Bajocco, 2011). The SQI is based on five parameters (texture, soil salinity, drainage, topsoil clay fraction and slope) proposed in the ESAI method. The soil data were acquired from the Harmonized World Soil Database at a 30 arc-second pixel resolution. The slope was computed using Shuttle Radar Topography Mission (SRTM) digital elevation data. The soil indicators and sensitivity scores are shown in Table 1. The SQI is often applied in small regions to reveal the spatial distribution of the soil quality. However, due to the lack of soil data coverage in Central Asia, soil indicators were regarded as static (variable). It is reasonable to assume only slight average soil quality changes on a large scale (Salvati et al., 2013; Tombolini et al., 2016). The formula used to calculate SQI is as follows (Kosmas et al., 1999):

$$SQI = (\text{texture} \times \text{soil salinity} \times \text{drainage} \times \text{topsoil clay fraction} \times \text{slope})^{1/5} \quad (1)$$

2.2.2. Climate quality index

The climate quality index (CQI) in the ESAI framework was assessed by three parameters: rainfall, aridity and aspect (Table 1), which affects the water use efficiency of natural vegetation. Global gridded precipitation data were derived from the Climatic Research Unit Datasets during 1992–2015 at a 0.5° resolution. These precipitation data have been derived from the spatially interpolated observation data of worldwide stations with homogeneity verification and good quality control (Mitchell and Jones, 2005). We obtained drought information from the globally standardized precipitation evapotranspiration index (*SPE*I) database. The *SPE*I database was developed using the FAO-56 Penman-Monteith method (Vicente-Serrano et al., 2015). The aspect was finally calculated by means of the SRTM digital elevation data. The CQI was measured as follows (Kosmas et al., 1999):

$$CQI = (\text{rainfall} \times \text{aridity} \times \text{slope aspect})^{1/3} \quad (2)$$

2.2.3. Vegetation quality index

The vegetation quality index (VQI) plays a crucial role in land degradation processes. The VQI was assessed through four indicators: erosion protection, fire risk, drought resistance and plant cover (Table 1). The first three indicators originated from the land cover maps provided by the European Space Agency from 1992 to 2015. The plant cover data at a spatial resolution of 1/12° were obtained from NOAA's Advanced Very High-Resolution Radiometer (AVHRR) data. The VQI was acquired using the geometric mean of the score values (Kosmas et al., 1999):

$$VGI = (\text{fire risk} \times \text{erosion protection} \times \text{drought resistance} \times \text{plant cover})^{1/4} \quad (3)$$

2.2.4. Management quality index

Different anthropogenic environmental pressures, which influence desertification vulnerability, were quantified with respect to agricultural intensity and policy enforcement (Table 1). Considering the data availability and specificity in Central Asia, an analysis of management quality was considered for croplands. Because the economy is dominated by agriculture and other activities is so limited in this region. The agricultural intensity and agricultural policy enforcement originated from the land cover maps provided by the European Space Agency. According to local agricultural systems and other similar studies (Prăvălie et al., 2017b), agricultural intensity can be categorized into three cases: low land use intensity, medium land use intensity and high land use intensity. Moreover, agricultural policy enforcement was assessed and classified into three cases: complete protection, partial protection and incomplete protection. The management quality index (MQI) was calculated as follows (Kosmas et al., 1999):

$$MQI = (\text{agricultural intensity} \times \text{policy enforcement})^{1/2} \quad (4)$$

2.2.5. Environmentally sensitive area index

Because of the limited dataset availability, the raster datasets of all parameters (Table S1, Supplementary material) were resampled to 1/12° and temporally assembled to the yearly values, which correspond to the medium spatial resolution of the plant cover dataset for the spatial analysis. In the study, a 24-year time period from 1992 to 2015 will be considered for further analysis.

A composite index known as the ESAI was calculated to monitor the sensitivity to desertification. ESAI was estimated as the geometric mean of four quality indexes in the ith space unit and jth year (Basso et al., 2000) as follows:

$$ESAI = \left(\mathrm{SQI}_{i,j} \times CQI_{i,j} \times VQI_{i,j} \times MQI_{i,j}\right)^{1/4} \quad (5)$$

Based on the adopted score system of the ESAI approach, the ESAI values varied from 1 (lowest sensitivity) to 2 (highest sensitivity) and were categorized into 4 main classes and 8 subclasses in this approach: (a) Non-affected (<1.17); (b) potential (1.17–1.22); (c) fragile 1 (1.23–1.26), fragile 2 (1.27–1.32), fragile 3 (1.33–1.37); and (d) critical 1 (1.38–1.41), critical 2 (1.42–1.53), critical 3 (>1.53) (Kosmas et al., 1999; Prăvălie et al., 2017b; Sneyers, 1991).

Despite the difficulty of validating a composite index, two indirect validations of desertification risk in Central Asia were conducted according to the spatial and temporal comparison of ESAI values, including (i) a quantitative analysis of the relationship between the ESAI and land use change between sparse vegetation and grasslands and (ii) a quantitative analysis of the relationship between the ESAI and net primary production (NPP).

The findings of a previous study confirmed that sparse vegetation is more sensitive to desertification than grasslands in the same region (Bajocco et al., 2012). Land use change between sparse vegetation and grasslands was identified, and ESAI values were extracted for the corresponding change pixels in 1992 and 2015, respectively. There are two behaviours identified in the correct assessment: when the areas were converted from sparse vegetation to grasslands, then the ESAI values were increased, indicating that land had increased sensitivity to desertification. When the areas were converted from grasslands to sparse vegetation, the ESAI values decreased, indicating that land had decreased sensitivity to desertification in this region.

Concerning the relationship between desertification and NPP, international initiatives, such as UNCCD and the Atlas initiative, have proposed that the desertification process can be indirectly tested by the change in NPP (Cherlet et al., 2018; Sommer et al., 2011). Furthermore, an increase in net primary productivity is a strategic indicator developed by UNCCD for desertification improvement. Therefore, a negative relationship should occur between ESAI and NPP during the time period; that is, the regions with increased NPP experience decreased land sensitivity to desertification.

2.3. Methods

2.3.1. Linear regression analysis

In the study, the SQI, CQI, VQI, MQI and ESAI dynamics were monitored using the linear regression analysis method. This method is a linear approach to model the relationship between an independent variable (year) and a dependent variable (indicator) (Seber and Lee, 2012). The slope coefficients of each pixel were obtained through the time series values of each pixel. The formula used to calculate the slope coefficients is as follows (Chatfield, 2016):

$$Slope = \frac{n\sum_{n}^{i=1} i \times X_i - \sum_{n}^{i=1} i \times \sum_{n}^{i=1} X_i}{n\sum_{n}^{i=1} i^2 - \left(\sum_{n}^{i=1} i\right)^2} \quad (6)$$

where *Slope* represents the change trend of each pixel in dependent variations, X_i is the value of the annual indicator in the ith year, i is the ith year, and n is the range of years in the study period.

2.3.2. Mann-Kendall test

The MK (Mann-Kendall) test recommended by the WMO (World Meteorological Organization) is robust in determining mutations for one continuous dataset (Yu et al., 2002). Currently, the MK test has been widely applied in meteorological and hydrological studies (Prăvălie et al., 2016; Prăvălie et al., 2019; Su et al., 2014). Based on the MK test, mutation years of the annual mean ESAI from 1992 to 2015 were identified to determine different time intervals for the further analysis of desertification risk. The main principles are as follows (Mann, 1945; Sneyers, 1991):

(1) The magnitude of the x_i ($i = 1,2, \ldots n$) annual time series is the data point in the ith year. Then, the Mann-Kendall test statistic is calculated as follows:

$$S = \sum_{k=1}^{n-1} \sum_{i=k+1}^{n} sign(x_i - x_k) \quad i = 1, 2, \cdots, n \tag{7}$$

$$\text{sign}(x_i\text{-}x_k) = \begin{cases} 1 & if \ x_i - x_k > 0 \\ 0 & if \ x_i - x_k = 0 \\ -1 & if \ x_i - x_k < 0 \end{cases} \tag{8}$$

(2) The variable statistics are calculated as follows:

$$UF_k = \frac{|S_k - E(S_k)|}{\sqrt{Var(S_k)}} \quad k = 1, 2, \cdots, n \tag{9}$$

$$E(S_k) = k(k-1)/4 \tag{10}$$

$$Var\,S_k = k(k-1)(2k+5)/72 \tag{11}$$

(3) The reversed variable statistics are defined as follows:

$$\begin{cases} UB_k = -UF_k \\ k = n + 1 - k \end{cases} \tag{12}$$

When curve UF_k and curve UB_k intersect between the two critical lines (±1.96), the intersected point is the mutation year. The mutation year is considered the beginning of change.

2.3.3. Convergence analysis

The convergence concept demonstrates a negative relationship between the differences in ESAI values over a particular time interval and the ESAI value in the initial year (Arbia and Paelinck, 2003). Convergence compares the average change over a time period to the initial ESAI value under the implicit assumption that all regions with the lowest value will change at a faster rate up to the mean ESAI value. In other words, a low ESAI value of the initial year is increased to the mean ESAI value in the corresponding area. This relationship also occurs if a high ESAI value of the initial year is decreased to the mean ESAI value in the corresponding area. Thus, a negative relationship occurs between the ESAI value at the end year and the ESAI value at the beginning year in all regions. The more negative the relationship, the more the ESAI values across all regions tend to converge around the mean value.

The average ESAI values were calculated for each administrative subdivision (Fig. S1, Supplementary material); subsequently, the average annual change rate during different time intervals was computed: 1992–2000, 2000–2008, and 2008–2015. The ordinary least squares (OLS) model was run using linear regression methods to measure the spatial convergence of ESAI for Central Asia. The convergence analysis was estimated as follows (Canetti and España, 1989; Tombolini et al., 2016):

$$\Delta ESAI_{(j1-j0,i)} = b_0 + b_1 \times ESAI_{(j0,i)} + \varepsilon \tag{13}$$

where $\Delta ESAI_{(j1\text{-}j0,\ i)}$ represents the change in ESAI over the corresponding time interval, $ESAI_{(j0,\ i)}$ represents the ESAI value in the ith spatial unit of the j_0th year and ε represents the error term. The significance of the coefficients (b_1) was judged at the 95% level using the F-tests. When coefficients are positive, the positive values indicate a divergence trend concerning the ESAI. When coefficients are negative, the negative values exhibit a convergence trend of ESAI (Tombolini et al., 2016).

To identify the spatiotemporal comparison of convergence patterns in ESAI, the geographically weighted regression (GWR) model was applied to estimate the spatially varying relations in the study (McMillen, 2004). The GWR model can estimate spatial coefficient values in each spatial unit by moving a weighted window. If the local coefficients are positive in space, the positive values indicate divergence patterns in the corresponding areas. If the local coefficients are negative in space, the negative values indicate convergence patterns in the corresponding areas.

2.3.4. Residual analysis

The residual analysis method was used to determine the relative importance of climate change and human activities in desertification risk (Evans and Geerken, 2004). The observed ESAI values were calculated using Eq. (5). The predicted ESAI values could be calculated based on the regression model between the annual ESAI and climatic factors (Wessels et al., 2012). Then, the ESAI residuals were acquired by the differences between the predicted and observed ESAI values for each pixel. According to the change trend of the ESAI residuals, the significance test can be categorized into two behaviours: when the change trend of the ESAI residuals was nonsignificant, the desertification risk could be explained by climate change. In contrast, when the change trend of the ESAI residuals was significant, the desertification risk could not be explained by climate change and may have been caused by human activities. This approach can effectively distinguish the driving factors of human activities from climate change regarding land sensitivity to desertification. The ESAI residuals were calculated as follows:

$$ESAI\ residuals = observed\ ESAI - predicted\ ESAI \tag{14}$$

3. Results

3.1. Spatial assessment of the quality indicators from 1992 to 2015

The spatial distribution and change trends of the four quality indexes from 1992 to 2015 are shown in Fig. 2. Significant spatial quality differences occurred between the annual mean index and change trend in Central Asia. The annual average CQI indicated that a high-quality state was found in the northern part of Kazakhstan, eastern Uzbekistan, Kyrgyzstan and Tajikistan, whereas a low-quality state was detected in the central part of Kazakhstan and the Ustyurt Plateau. The overall change in CQI showed that most areas experienced a significant decreasing trend. However, a significant increasing CQI trend was observed in the Ustyurt Plateau and Uzbekistan, with change rates amounting to 0.007/a.

The VQI assessment showed that a low-quality state was noticeable in the southern part of Central Asia with the exception of Kyrgyzstan and

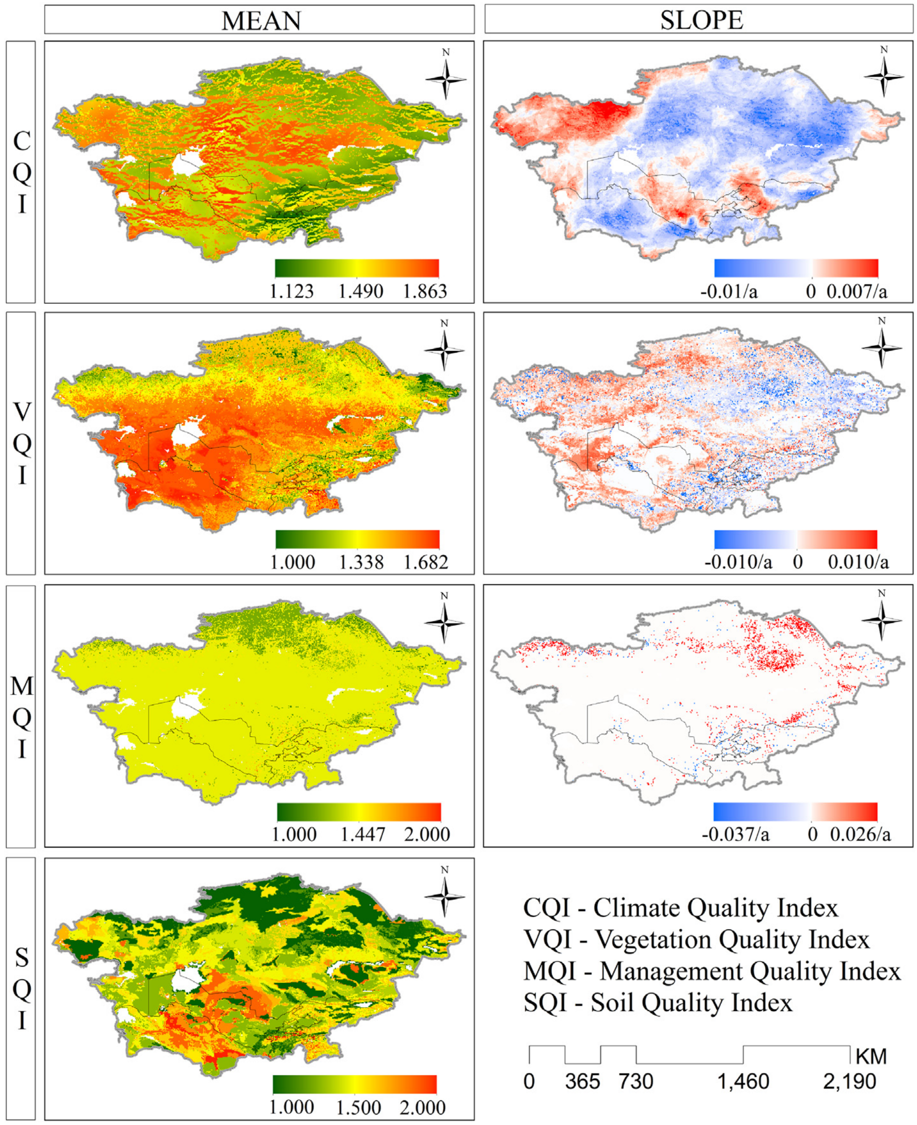

Fig. 2. Spatial distribution and change trends of the four quality indicators (CQI, VQI, MQI and SQI) from 1992 to 2015.

Tajikistan, which showed a moderate quality, whereas high- and moderate-quality states were observed in the northern part of Kazakhstan. The change rates of the annual VQI ranged from −0.01/a to 0.01/a. The VQI showed opposite spatial trends between the eastern part (decreasing trend) and western part (increasing trend). Only small, scattered areas were characterized as being in very high-quality states.

In the case of MQI, northern Kazakhstan was prone to being low quality. This result is mainly because of the higher density of natural vegetation and rainfed croplands in this area than in other areas. Most regions suffered from moderate quality. Small scattered areas with high and low quality were identified due to land use change. In the past 20 years, the MQI remained stable during the study period. The northeastern part of Kazakhstan has experienced an increased MQI trend, whereas the opposite tendencies have been identified in eastern Uzbekistan.

In terms of SQI, a noteworthy increased has occurred from north to south, with a higher quality detected in northern Kazakhstan and a lower quality in the Aral Sea basin. This result may be caused by the synergistic effect of the soil salinity, texture and topsoil clay fraction.

3.2. Spatial assessment of ESAI from 1992 to 2015

The spatial representation of the mean ESAI from 1992 to 2015 (Fig. 3a) showed different degrees of susceptibility to desertification. The results revealed that low values of the average ESAI occurred in northern Kazakhstan and mountainous regions, with a mean ESAI as low as 1.112. Notably, the high values were especially concentrated in the Karakum and Kyzylkum Deserts, with mean ESAIs of 1.601. The results are consistent with our understanding that desertification sensitivity in the desert areas is higher than that in hilly and mountainous districts. Based on the linear regression analysis method and F test of the change trend, the overall change trends with significant changes in ESAI are determined, and they are shown in Fig. 3b. Most regions showed a slightly decreasing trend in the average ESAI over the past two decades. However, the significantly increasing tendency in the Ustyurt Plateau, Uzbekistan and Turkmenistan cannot be ignored (with annual change rates of up to 0.003/a). Thus, ESAI changes in Central Asia demonstrate significant regional characteristics.

It is crucial to validate the ESAI methodology in Central Asia. According to land use changes between sparse vegetation and grasslands, 622 pixels were converted from sparse vegetation to grasslands, and 172 pixels were converted from grasslands to sparse vegetation (Fig. S3, Supplementary material). Approximately 85.80% of the pixels were correctly identified via assessments of desertification risk in these two land use change types. Furthermore, a definite negative correlation exists between the ESAI change and NPP change from 2008 to 2014, with a high R^2 of up to 0.53 (Fig. S3, Supplementary material). This finding suggests

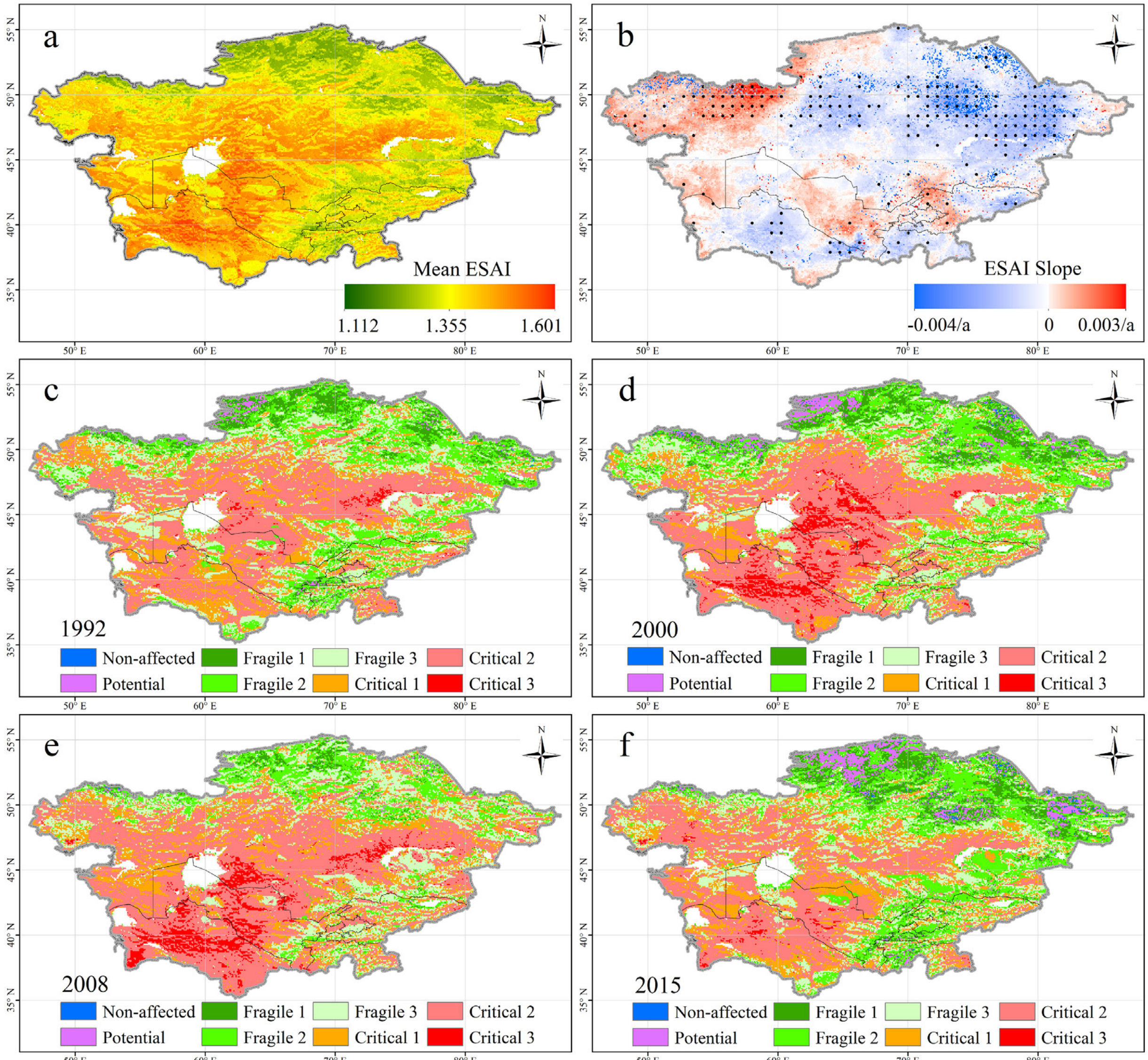

Fig. 3. Spatial distribution and ESAI change trends. (a) Spatial distribution of the mean ESAI from 1992 to 2015; (b) annual change trends in ESAI; (c), (d), (e) and (f) spatial distribution of the classified ESAI in 1992, 2000, 2008 and 2015, respectively. The black spots show the significant change trends in ESAI.

that the ESAI framework produces a sensible desertification risk assessment result. In addition, field investigations (2015) indicated that the desertification difference among field observations was consistent with the results of the corresponding classified ESAI among different sites (Fig. S4, Supplementary material). Land sensitivity to desertification was higher in Uzbekistan than in Kyrgyzstan and Tajikistan. Thus, the result of the ESAI approach is reliable in Central Asia.

The mutation results of the annual mean ESAI tested by the MK method are shown in Fig. 4. Curve UF_k and curve UB_k intersected between critical lines (± 1.96) in approximately 1993, 2000 and 2008, which indicated that some abrupt points were found during these years. Due to the abrupt point in approximately 1993 near the beginning of the study period, three time intervals (1992–2000, 2000–2008 and 2008–2015) were chosen to study land sensitivity to desertification and explore convergence.

The ESAI maps for 1992, 2000, 2008 and 2015 are displayed in Fig. 3c–f. According to these maps, the vast majority of fragile classes were distributed in the northern part of Central Asia, and the majority of critical classes (especially critical 2) were found in south Central Asia during both periods. Moreover, Uzbekistan and Turkmenistan were more sensitive to desertification than other regions, especially in 2008. Table 2 shows the statistical area and percentage of each sensitivity class in ESAI. The proportions of the fragile classes varied over time, decreasing vastly from 46.28% in 1992 to 33.27% in 2008 while increasing to 48.28% in 2015 in the subsequent time span (2008–2015). Considering the critical classes, the maximum percentage (66.34%) was observed in 2008. Between 1992 and 2008, nearly 13.66% of the study area fell into the critical classes, which were relatively concentrated in the eastern part of Central Asia. However, the areas in critical classes 2 and 3 decreased by 58.46×10^4 km^2 and 19.89×10^4 km^2 in 2015, respectively, and the level of desertification sensitivity was lower than that in 1992. The non-affected and potential classes were scattered in the fragile classes in northern Central Asia, with the highest percentages observed in 2008 at values of 0.42% and 4.66%, respectively. In general, Central Asia gradually became more sensitive to desertification in 2008 (than in 1992) and improved after 2008.

The mutation years for each pixel were detected using the MK test (Mann, 1945; Sneyers, 1991). According to the results, the spatial distribution of mutation years was obtained and can be classified into stable or consistent ($P < 0.05$) and inconsistent ($P > 0.05$) changes. The results showed that the areas with stable or consistent changes were distributed in most areas and relatively concentrated in the southern part of

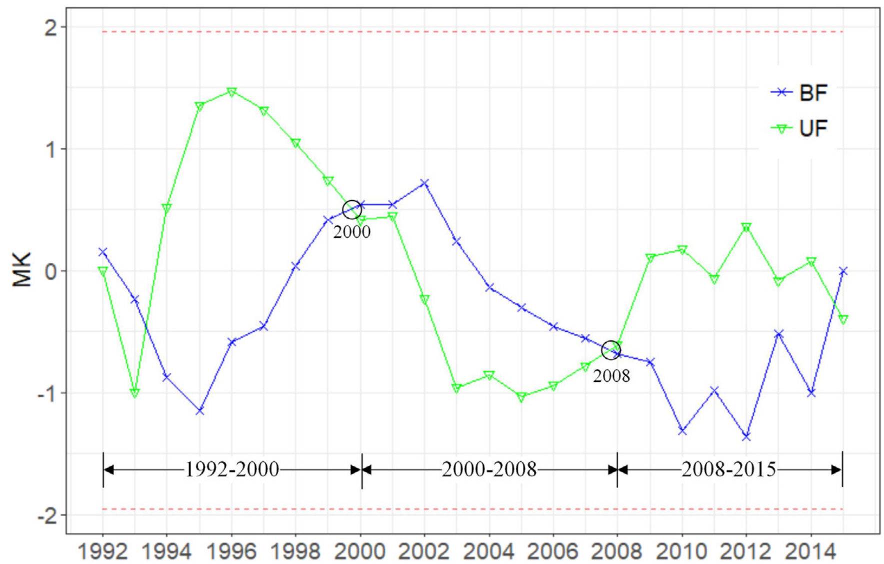

Fig. 4. Mutation results of the annual mean ESAI from 1992 to 2015.

the study area. For areas showing an inconsistent change, the spatial distribution of mutation year detection was classified into three periods (1992–2000, 2001–2008 and 2009–2015) (Fig. 5a). This classification proved that many pixels with mutation years from 2009 to 2015 were scattered in the northern part of Kazakhstan, whereas most pixels with mutation years from 2001 to 2008 were relatively concentrated in eastern Kazakhstan. During the study period, the Aral Sea basin and Kazakhskiy Melkosopochnik had more pixels with mutation years from 1992 to 2000 than other regions.

The statistical results of the mutation years for various countries were compared (Fig. 5b). The mutation year proportions during different time periods varied among different countries. The highest percentage of mutation years (45.32%) under stable and consistent change was observed in Kazakhstan, followed by Kyrgyzstan. In contrast, Tajikistan and Turkmenistan accounted for 48.96% and 66.76% of the pixels, respectively, and possessed the highest proportions of mutation years during the first period. Considering the mutation years in the second period, a high percentage was identified in Uzbekistan and Tajikistan, including >25.94% of the pixels in Uzbekistan. The pixels with mutation years in the third period were mainly noticed in Kazakhstan, with a proportion of up to 18.60%. In other countries, the classification percentages were <5%. The proportion of mutation years during different periods in Central Asia decreased in the following order: stable and consistent change, first period (1992–2000), second period (2001–2008) and third period (2009–2015). The results indicated that some driving factors for desertification sensitivity in different regions may have changed, which results in the sensitivity moving in various directions, especially during the first period.

3.3. Convergence analysis of the ESAI level

The spatial convergence analysis coefficient estimates of the administrative subdivision spatial scale are illustrated in Table S2 (Supplementary material). The convergence model was used to study the relation between the ESAI at the beginning of the studied time intervals (1992, 2000, and 2008) and the difference over three respective time periods (1992–2000, 2000–2008, and 2008–2015). The convergence coefficient during the period from 1992 to 2000 was positive (0.130) and had a significant Spearman's nonparametric correlation coefficient, which suggested a tendency to diverge. The convergence coefficients over the subsequent time intervals (2000–2008 and 2008–2015) were negative (−0.534, −0.268) with the high adjusted R^2, which indicated that the ESAI environmental conditions tended to converge at that time. The findings are consistent with the results of the mutation year detection. From 1992 to 2000, more pixels with mutation years were observed. The environmental conditions in the recent time intervals were, therefore, more stable than those in the first time interval.

Based on the GWR model, the spatial distribution of the spatial convergence analysis parameters in ESAI based on three time intervals are shown in Fig. 6. Most parts of Central Asia with positive ESAI coefficients showed divergence from 1992 to 2000. The impact of the district's divergence is higher in the northwest regions than elsewhere in Central Asia. A high adjusted R^2 was observed in these areas. For 2000–2008, negative ESAI coefficients were concentrated in northern Central Asia with a high adjusted R^2, whereas positive ESAI coefficients were seen in Uzbekistan and Turkmenistan with a low adjusted R^2. This result indicated that the ESAIs tend to converge in the northern districts and

Table 2
Statistical areas and percentages of different ESAI sensitivity degrees.

Class	Sub-class	1992		2000		2008		2015	
		x10^4 km^2	%	x10^4 km^2	%	x10^4 km^2	%	x10^4 km^2	%
Non-affected	N	0.21	0.05	1.03	0.26	0.11	0.03	1.63	0.42
Potential	P	3.88	1.00	11.54	2.96	1.41	0.36	18.13	4.66
Fragile	F1	23.54	6.05	26.92	6.92	8.22	2.11	32.33	8.30
	F2	70.62	18.14	64.79	16.64	44.05	11.32	80.69	20.73
	F3	85.99	22.09	70.23	18.04	77.25	19.84	74.94	19.25
Critical	C1	76.73	19.71	54.56	14.01	67.67	17.38	69.35	17.81
	C2	125.53	32.24	139.95	35.95	168.43	43.27	109.97	28.25
	C3	2.80	0.72	20.28	5.21	22.16	5.69	2.27	0.58

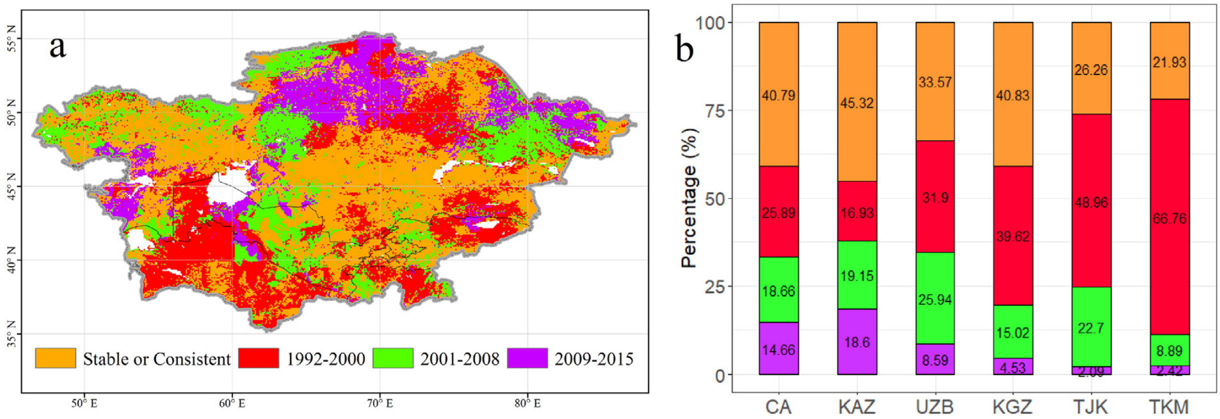

Fig. 5. Spatial distribution of mutation years classified into three periods (a) and statistical results of the mutation years for different countries (b). CA: Central Asia; KAZ: Kazakhstan; UZB: Uzbekistan; KGZ: Kyrgyzstan; TJK: Tajikistan; TKM: Turkmenistan. The legend is the same for (b) and (a).

diverge in the southern districts. The negative ESAI coefficients were revealed in most areas of Central Asia for 2008–2015, especially in the eastern districts with a high adjusted R^2. Positive ESAI coefficients were found in the Ustyurt Plateau in this period. In general, desertification sensitivity tended to diverge between 1992 and 2000 and converge in subsequent time periods. The ESAIs converged or diverged more rapidly in the high land quality districts than the low land quality districts.

3.4. Relative roles of climate change and human activities in desertification risk

Based on a linear regression analysis method and F test of the change trend, the spatial distribution of climatic change trends according to the significance test in the three time intervals is demonstrated in Fig. 7a–f. In recent decades, Central Asia has experienced significant precipitation and temperature changes in some regions. Precipitation in most regions presented different trends during the different time periods, with significant decreasing trends found in southern Central Asia for 1992–2000 and in northern Central Asia for 2000–2008 (Fig. 7a and b) and increasing trends observed for 2008 to 2015 in most regions (Fig. 7c). The temperatures showed a clear upward trend in the southern part of Central Asia, with the greatest change rate being 0.28 °C/a, which was observed from 1992 to 2000 (Fig. 7d). Overall, the study area experienced a rapid and accelerated warming and drying trend from 1992 to 2008. However, it became warmer and moister after 2008.

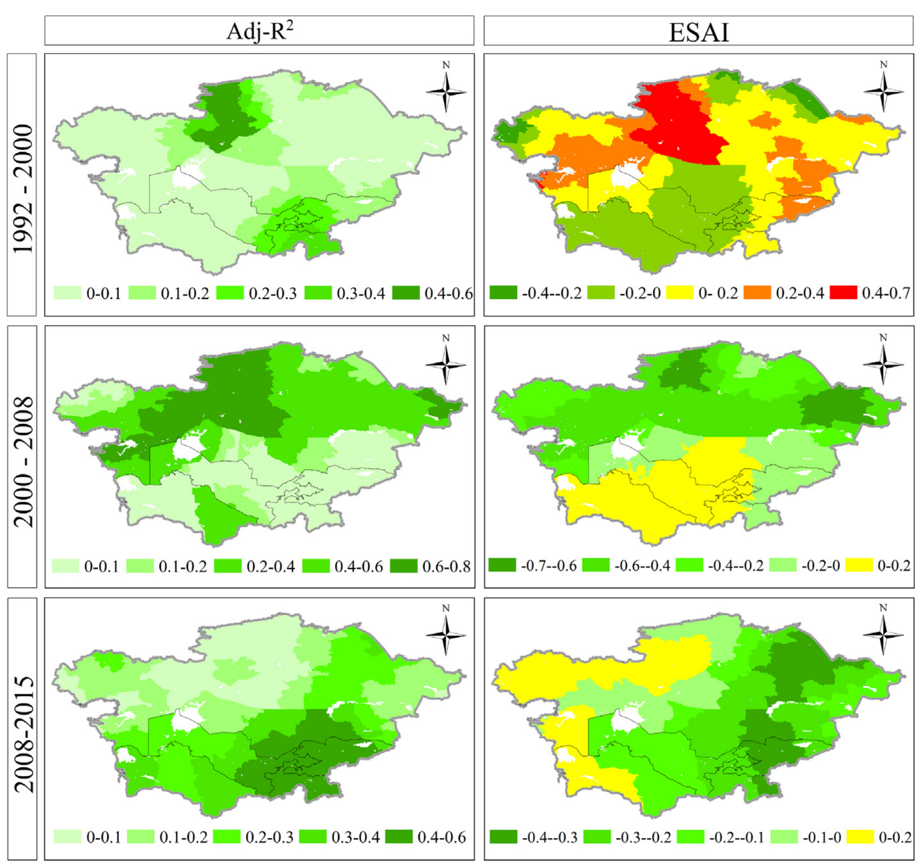

Fig. 6. GWR model for ESAI spatial convergence analysis by time interval in Central Asia.

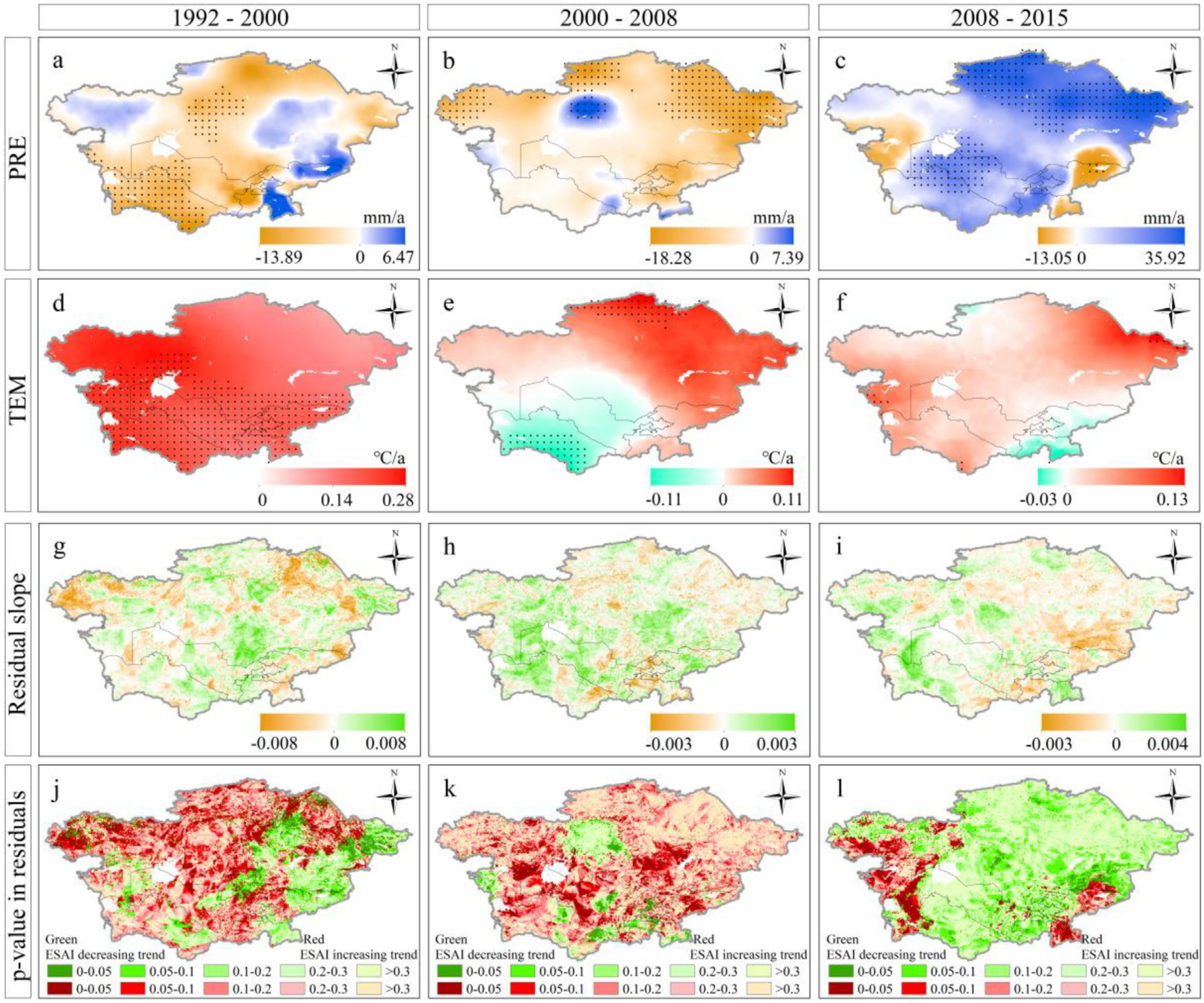

Fig. 7. Spatial distributions of precipitation and temperature change trends (a–f). The black spots show the significant change trends in the climatic factors using the F test. (g–i) show the overall trends of the ESAI regression residuals based on the regression model between the annual ESAI and climatic factors. (j–l) show overlay results of significant changes (*P*-value) in ESAI residuals and the ESAI change trends. The dark green and dark red shading show that the significant changes in the ESAI residuals could not be explained by climatic trends and were mainly caused by human activities, whereas the light green and light red shading show that nonsignificant changes in the ESAI residuals could be explained by climatic trends.

To explore the relative effects of climate change and human activities on desertification risk, the overall trends of the ESAI regression residuals were calculated for different time intervals (Fig. 7g–i). The results showed that the change trends in the ESAI residuals for 1992–2000 in northern Kazakhstan were higher than the subsequent time intervals (2000–2008 and 2008–2015). Significant changes (*P*-value) in ESAI residuals and the ESAI change trend were superimposed (Fig. 7j–l). For 1992–2000, dark red shading with significant (*P*-value <0.05) ESAI residuals and an increasing ESAI trend are mainly located in northern Central Asia, whereas areas with dark green shading showing the significance of ESAI residuals and a decreasing ESAI trend are scattered in eastern Central Asia. Climatic fluctuations could not be illustrated in these regions; thus, changes were mainly caused by anthropogenic disturbances. However, considering 2000–2008 and 2008–2015, most areas with light red or light green shading showing a nonsignificant change in ESAI residuals can be explained by climate change. An increasing trend in the average ESAI was identified in most regions from 2000 to 2008. However, a decreasing tendency was found from 2008 to 2015. Other than climatic drivers of desertification risk, the Aral Sea basin during 2000–2008 experienced an increasing ESAI trend with dark red shading, which was mainly triggered by human activities. The same phenomenon was observed on the Ustyurt Plateau from 2008 to 2015.

4. Discussion

4.1. Spatial convergence patterns from 1992 to 2000

Based on a wide dataset covering Central Asia, the direction of desertification risk during different time periods was explored in this study. Traditional methods have been used to monitor desertification risk in Central Asia based on trend analyses of vegetation indexes throughout the study period (Hill et al., 2008; Kundu and Dutta, 2011). In the transitional ecotone, which ignored the desertification process, the mutation years could not be detected under the effects of external disturbance. In this study, the statistical analyses using both the Mann-Kendall test and convergence analysis guaranteed the reliability of the desertification risk direction. Abrupt change years (2000 and 2008) were detected among the three time intervals (1992–2000, 2000–2008 and 2008–2015), which is consistent with the results of previous studies (Stulina and Eshchanov, 2013; Zhang et al., 2017). Stulina and Eshchanov, 2013 reported that extreme dry spells were observed in 2000 and 2008.

The spatial convergence analysis observed in Central Asia reflects the complex interactions between changes in the ecological conditions and socioeconomic context over the different time intervals (Safriel and Tal, 2010; Yang et al., 2013). For 1992–2000, the analysis identified

desertification risk divergence patterns over the first time interval, especially in the northern part of Central Asia (Table S2, Supplementary material and Fig. 6). This finding could be explained by the effects of the Soviet Union collapse in 1991. The socioeconomic and political development of different countries underwent diverse levels of change, resulting in the abandonment of extensive cultivated fields, which were converted to derelict lands in northern Kazakhstan, and the collapse of animal husbandry in eastern Kazakhstan (Klein et al., 2012; Xi and Sokolik, 2016). Thus, the desertification risk during this period was bound to be influenced by the spatial diversifications in the manner and scale of human activities (Hostert et al., 2011; Zhou et al., 2015b). Desertification risk divergence patterns were identified in northern Kazakhstan (Fig. 6) with regard to cropland abandonment from 1992 to 2000. After the Soviet Union collapsed in 1991, because of the reduced agricultural subsidies and insecure land tenure (Zhou et al., 2015b), 4.89 million hectares of cultivated land were abandoned in Kazakhstan (Fig. S5, Supplementary material), especially in northern Kazakhstan. Vegetation recovery was difficult over a short time period in arid regions, and many croplands were transformed into sparse vegetation, resulting in surface soil exposure. Exposed surface soil exacerbated the sensitivity to desertification in northern Kazakhstan (Mirzabaev et al., 2016). This finding can be confirmed by the results of the ESAI residuals analysis. Northern Kazakhstan underwent an increasing ESAI trend indicated by dark red shading, and it was mainly triggered by human activities during this period (Fig. 7j).

The ESAI divergence patterns in eastern Kazakhstan, Kyrgyzstan and Tajikistan (Fig. 6) were related to pasture abandonment from 1992 to 2000. After the Soviet Union collapsed, the funding for animal husbandry vanished with the political independence of the different nations (Karnieli et al., 2008) compared with the heavy funding received during the former Soviet Union. Livestock profits were greatly reduced, leading to the collapse of animal husbandry in Kazakhstan, Kyrgyzstan and Tajikistan, and livestock inventories were recorded to decrease by 62.90%, 44.12% and 31.01%, respectively (Fig. S5, Supplementary material). Thus, summer and remote rangelands were abandoned, and overgrazing was alleviated in these areas. As pasture recovery progressed, land sensitivity to desertification decreased (Hauck et al., 2016; Robinson, 2016b). The potential reason for the divergence patterns in these regions is consistent with the result of the ESAI residuals analysis, which showed the significance of ESAI residuals and decreasing ESAI trend located mainly in eastern Central Asia (Fig. 7j). Robinson et al. (Robinson, 2016a) also reported that the desertification reversion of grasslands was related to decreased livestock inventories in these regions during the post-Soviet period. The convergence patterns in the deserts of southern Central Asia from 1992 to 2000 (Fig. 6) can be explained by decreased precipitation and increased temperature, which changed significantly according to the ESAI residuals analysis over this period (Fig. 7a, d and j) and resulted in an increased sensitivity to desertification in the deserts. The sparse vegetation is distributed in these areas, and the growth is dependent upon precipitation rather than irrigation. In this case, the spatial convergence pattern can be regarded as an early warning of desertification risk (Tombolini et al., 2016).

4.2. Spatial convergence patterns from 2000 to 2015

Due to the stabilization of environmental conditions after a few years, convergence patterns were observed in most regions over the subsequent time intervals (2000–2008 and 2008–2015) (Fig. 6). For 2000–2008, most areas became increasingly sensitive to desertification with the convergence pattern caused by decreased precipitation (Figs. 6, 7b and k), especially in northern Central Asia, which is consistent with previous studies (Stulina and Eshchanov, 2013; Zhou et al., 2015b). Zhang et al. demonstrated that grassland desertification was significantly affected by decreased precipitation in this region (Zhang et al., 2017). In this sense, specific adaptation strategies should be adopted in districts where the ESAI convergence has changed rapidly. However, the divergence pattern in the Aral Sea basin cannot be ignored and may be caused by human activities (Figs. 6 and 7k). The reduction in runoff from the upstream areas of rivers can affect the available ecological water in the downstream areas during the dry years of 2000 and 2008, especially in the Amu Darya River delta (Fig. S6, Supplementary material), resulting in an increased sensitivity to desertification in some regions (Fig. 7k), as shown in a previous study (Dubovyk et al., 2013). Furthermore, as a result of the consistent recession of the Area Sea, the large Aral Sea was divided into the eastern and western Aral Seas in 2006. The area, level and volume of the large Aral Sea decreased by 61.60%, 14.63% and 74.72% from 2000 to 2008, respectively (Fig. S6, Supplementary material). Subsequently, some lands were significantly degraded and became highly sensitive to desertification in the wetland delta (Fig. 7k). Asarin et al. also reported that the hydrographic network and landscapes in this region have undergone severe degradation because of the dramatic reduction in river inflow (Asarin et al., 2010). Therefore, the divergence pattern of the Aral Sea basin was found and cannot be explained by regional climate change (Fig. 7k).

From 2008 to 2015, convergence patterns were found in most regions with regard to augmented precipitation (Figs. 6, 7c and l). Although precipitation could increase the risk of water erosion-induced desertification, precipitation was beneficial for vegetation growth, especially in the drylands (Zhao et al., 2011), which resulted in decreased sensitivity to desertification in most parts of Central Asia. The ESAI residuals analysis confirmed that decreased sensitivity could be explained by climate change (Fig. 7l). Moreover, the low sensitivity areas in eastern Central Asia were more likely to converge by increased precipitation (Fig. 6). Concerning the western part of the Ustyurt Plateau, the divergence patterns were caused by gas and oil reserve exploitation with an increasing trend of desertification risk (Figs. 6 and 7l). Many more oil and gas wells were spatially concentrated and heavily developed in this region. Subsequently, the increased number of heavy-duty vehicles used in oil and gas exploitation negatively affected the vegetation cover state (Khabibullo et al., 2017), which may illustrate the observed divergence patterns caused by human activities (Fig. 7l).

Spatial convergence is an economic concept. The combination of convergence patterns and desertification risk is another advance in the technical perspective of this study. The desertification process presents heterogeneously changes that lead to different convergence patterns in land sensitivity to desertification among different regions. In other words, the convergence processes have gradually increased the desertification risk gap among the high and low sensitivity districts (Bajocco et al., 2015; Tombolini et al., 2016). From 1992 to 2000, the average ESAI diverged in northern Central Asia, which has been in a moderately high land quality state. The average ESAI converged in the low land quality areas (vegetation, soil and climate), including the Muyunkun, Karakum and Kyzylkum Deserts of southern Central Asia, which showed lower spatial heterogeneity than northern Central Asia (Fig. 6). Thus, the vulnerable zones tend to converge, and the low sensitivity areas tend to diverge during this time interval. However, convergence patterns in most parts of Central Asia were found over the following two time intervals: 2000–2008 and 2008–2015. The low sensitivity areas demonstrated convergence patterns. In this sense, the findings of our study suggest that spatial convergence and divergence have some potential explanations. Previous studies also indicated that the ESAI spatial convergence is closely linked to the different drivers of desertification (Basso et al., 2012; Tombolini et al., 2016). Furthermore, the convergence process during the different time periods was verified for consistency by the results of the mutation year detection in ESAI for each pixel over the study period. Notably, the proportion of mutation years found between 1992 and 2000 was higher than that of the other time intervals.

5. Conclusions

In this study, the desertification sensitivity in Central Asia was monitored using the ESAI methodology from 1992 to 2015. Combined with

the spatial convergence analysis, we investigated the ESAI convergence processes as revealed by an early warning of desertification risk and performed a spatiotemporal comparison of convergence patterns based on different time intervals. The main results are summarized as follows:

(1) Low average ESAI values were observed in northern Kazakhstan and mountainous regions, with mean ESAI values as low as 1.112, whereas high values were concentrated in the Kyzylkum and Karakum Deserts, with mean ESAIs of 1.601. Desertification risk gradually increased in 2008 (more than in 1992) and improved after 2008. The convergence analysis revealed that the desertification sensitivity trend diverged between 1992 and 2000 and converged over the subsequent time periods (2000–2008 and 2008–2015) in most regions of Central Asia. Furthermore, the ESAIs converged or diverged more rapidly in the high land quality districts than in the low land quality districts.

(2) Spatial convergence and divergence are related to climate change and human activities, respectively. The ESAI divergence patterns over 1992–2000 were caused by the collapse of the Soviet Union in 1991. The socioeconomic and political development models between different countries underwent various levels of change. The desertification risk divergence patterns in northern Central Asia were associated with cropland abandonment and pasture abandonment. Notably, a higher proportion of mutation years was found between 1992 and 2000 than during any other time interval.

(3) In contrast, the ESAI convergence patterns from 2000 to 2008 and 2008–2015 occurred with precipitation change. In 2000–2008, most areas experienced increased desertification sensitivity with the convergence pattern caused by decreased precipitation, especially in northern Central Asia. In this sense, specific adaptation strategies should be adopted in districts where the ESAI convergence has rapidly changed. However, for the time interval of 2008–2015, convergence patterns were found in most regions with regard to the augmented precipitation, which resulted in decreased desertification sensitivity. Moreover, the low sensitivity areas were more likely to converge under increased precipitation.

The combination of convergence patterns and desertification risk represents an advance in the technical perspective of this study. Desertification risk is a very complicated process caused by multiple factors. Data availability and access management quality indicators remain the primary concerns for developing increased spatial precision. In future investigations, more economic and environmental indicators are required to obtain a deeper understanding of desertification risk and convergence in Central Asia.

Acknowledgements

We would like to express our sincere gratitude to the European Space Agency, NASA and United Nations Environment for providing the indicator dataset. We thank the Harmonized World Soil Database of the Food and Agriculture Organization for providing the gridded soil dataset. We also acknowledge the Climatic Research Unit (University of East Anglia) for sharing the latest version of the Climatic Research Unit Version 4.02 (CRU TS4.02) from their website at http://www.cru.uea.ac.uk/data/. This research was supported by the Strategic Priority Research Program of Chinese Academy of Sciences [Grant No. XDA20030101].

Author contributions

Anming Bao designed the research. Liangliang Jiang processed the data, analysed the results and wrote the manuscript. Guli·Jiapaer, Guoxiong Zheng, Khusen Gafforov, Alishir Kurban and Philippe De Maeyer provided analysis tools and technical assistance. All authors contributed to the final version of the manuscript through proofreading and by providing constructive ideas.

Conflicts of interest

The authors declare no conflicts of interest.

Appendix A. Supplementary data

Supplementary data to this article can be found online at https://doi.org/10.1016/j.scitotenv.2018.12.152.

References

Arbia, G., Paelinck, J.H., 2003. Spatial econometric modeling of regional convergence in continuous time. Int. Reg. Sci. Rev. 26, 342–362.

Asarin, A.E., Kravtsova, V.I., Mikhailov, V.N., 2010. Amudarya and Syrdarya Rivers and Their Deltas. Springer, Berlin Heidelberg.

Assessment ME, 2005. Ecosystems and human well-being: desertification synthesis. Millennium Ecosystem Assessment.

Bajocco, S., De Angelis, A., Perini, L., Ferrara, A., Salvati, L., 2012. The impact of land use/land cover changes on land degradation dynamics: a Mediterranean case study. Environ. Manag. 49, 980–989.

Bajocco, S., Salvati, L., Smiraglia, D., Ceccarelli, T., Perini, L., 2015. Planning for sustainable agro-forest systems: protected areas and soil degradation hotspots in Italy (1990–2010). Soil Sci. Plant Nutr. 61, 404–413.

Bakr, N., Weindorf, D.C., Bahnassy, M.H., El-Badawi, M.M., 2012. Multi-temporal assessment of land sensitivity to desertification in a fragile agro-ecosystem: environmental indicators. Ecol. Indic. 15, 271–280.

Barro, R.J., Sala-I-Martin, X., 2004. Economic Growth. 2nd edition. MIT Press, Cambridge, MA.

Basso, F., Bove, E., Dumontet, S., Ferrara, A., Pisante, M., Quaranta, G., et al., 2000. Evaluating environmental sensitivity at the basin scale through the use of geographic information systems and remotely sensed data: an example covering the Agri basin (southern Italy). Catena 40, 19–35.

Basso, B., De Simone, L., Cammarano, D., Martin, E., Margiotta, S., Grace, P., et al., 2012. Evaluating responses to land degradation mitigation measures in southern Italy. Int. J. Environ. Res. 6, 367–380.

Becerril-Piña, R., Mastachi-Loza, C.A., González-Sosa, E., Díaz-Delgado, C., Bâ, K.M., 2015. Assessing desertification risk in the semi-arid highlands of central Mexico. J. Arid Environ. 120, 4–13.

Behnke, R., Mortimore, M., 2016. The End of Desertification? Springer, Berlin Heidelberg

Bohovic, R., 2016. The spatial and temporal dynamics of remotely-sensed vegetation phenology in central Asia in the 1982–2011 period. Eur. J. Remote Sens. 279.

Canetti, R.M., España, M.D., 1989. Convergence analysis of the least-squares identification algorithm with a variable forgetting factor for time-varying linear systems. Automatica 25, 609–612.

Chatfield, C., 2016. The Analysis of Time Series: An Introduction. CRC Press.

Cherlet, M., Hutchinson, C., Reynolds, J., Hill, J., Sommer, S., von Maltitz, G., 2018. World Atlas of Desertification. Publication Office of the European Union, Luxembourg https://doi.org/10.2760/0629.

Contador, J.F.L., Schnabel, S., Gutiérrez, A.G., Fernández, M.P., 2009. Mapping sensitivity to land degradation in Extremadura. SW Spain. Land Degrad. Dev. 20, 129–144.

Davi, N.K., D'Arrigo, R., Jacoby, G.C., Cook, E.R., Anchukaitis, K.J., Nachin, B., et al., 2015. A long-term context (931–2005 C.E.) for rapid warming over Central Asia. Quat. Sci. Rev. 121, 89–97.

de Beurs, K.M., Henebry, G.M., Owsley, B.C., Sokolik, I., 2015. Using multiple remote sensing perspectives to identify and attribute land surface dynamics in Central Asia 2001–2013. Remote Sens. Environ. 170, 48–61.

D'Odorico, P., Bhattachan, A., Davis, K.F., Ravi, S., Runyan, C.W., 2013. Global desertification: drivers and feedbacks. Adv. Water Resour. 51, 326–344.

Dubovyk, O., Menz, G., Conrad, C., Kan, E., Machwitz, M., Khamzina, A., 2013. Spatio-temporal analyses of cropland degradation in the irrigated lowlands of Uzbekistan using remote-sensing and logistic regression modeling. Environ. Monit. Assess. 185, 4775–4790.

Evans, J., Geerken, R., 2004. Discrimination between climate and human-induced dryland degradation. J. Arid Environ. 57, 535–554.

Ezcurra, R., 2007. Is there cross-country convergence in carbon dioxide emissions? Energy Policy 35, 1363–1372.

Farajzadeh, M., Egbal, M.N., 2007. Evaluation of MEDALUS model for desertification hazard zonation using GIS; study area: Iyzad Khast plain, Iran. Pak. J. Biol. Sci. 10, 2622–2630.

Fleskens, L., Stringer, L.C., 2014. Land management and policy responses to mitigate desertification and land degradation. Land Degrad. Dev. 25, 1–4.

Gessner, U., Naeimi, V., Klein, I., Kuenzer, C., Klein, D., Dech, S., 2013. The relationship between precipitation anomalies and satellite-derived vegetation activity in Central Asia. Glob. Planet. Chang. 110, 74–87.

Giannias, D., Liargovas, P., Manolas, G., 1999. Quality of life indices for analysing convergence in the European Union. Reg. Stud. 33, 27–35.

Guo, H., Bao, A., Liu, T., Ndayisaba, F., Jiang, L., Kurban, A., et al., 2018a. Spatial and temporal characteristics of droughts in Central Asia during 1966–2015. Sci. Total Environ. 624, 1523–1538.
Guo, H., Bao, A., Ndayisaba, F., Liu, T., Jiapaer, G., El-Tantawi, A.M., et al., 2018b. Space-time characterization of drought events and their impacts on vegetation in Central Asia. J. Hydrol. 564, 1165–1178.
Han, Q., Luo, G., Li, C., Shakir, A., Wu, M., Saidov, A., 2016. Simulated grazing effects on carbon emission in Central Asia. Agric. For. Meteorol. 216, 203–214.
Hauck, M., Artykbaeva, G.T., Zozulya, T.N., Dulamsuren, C., 2016. Pastoral livestock husbandry and rural livelihoods in the forest-steppe of east Kazakhstan. J. Arid Environ. 133, 102–111.
Hill, J., Stellmes, M., Udelhoven, T., Röder, A., Sommer, S., 2008. Mediterranean desertification and land degradation. Glob. Planet. Chang. 64, 146–157.
Xu, H.-j, Wang, X.-p., Zhang, X-x, 2016. Decreased vegetation growth in response to summer drought in Central Asia from 2000 to 2012. Int. J. Appl. Earth Obs. Geoinf. 52, 390–402.
Hooke, J.M., Brookes, C.J., Duane, W., Mant, J.M., 2005. A simulation model of morphological, vegetation and sediment changes in ephemeral streams. Earth Surf. Process. Landf. 30, 845–866.
Hostert, P., Kuemmerle, T., Prishchepov, A., Sieber, A., Lambin, E.F., Radeloff, V.C., 2011. Rapid land use change after socio-economic disturbances: the collapse of the Soviet Union versus Chernobyl. Environ. Res. Lett. 6, 045201.
Jiang, L., Guli, Jiapaer, Bao, A., Guo, H., Ndayisaba, F., 2017. Vegetation dynamics and responses to climate change and human activities in Central Asia. Sci. Total Environ. 599–600, 967–980.
Karnieli, A., Gilad, U., Ponzet, M., Svoray, T., Mirzadinov, R., Fedorina, O., 2008. Assessing land-cover change and degradation in the central Asian deserts using satellite image processing and geostatistical methods. J. Arid Environ. 72, 2093–2105.
Khabibullo, S., Bekhzod, A., Tashkhonim, R., Nodira, R., Rapat, A., Yusuf, V., 2017. Some notes on the key botanical territories of Ustyurt (Uzbekistan) and the influence of oil and gas industries on them. Am. J. Plant Sci. 08, 2811–2824.
Kienzler, K., Lamers, J., McDonald, A., Mirzabaev, A., Ibragimov, N., Egamberdiev, O., et al., 2012. Conservation agriculture in Central Asia—what do we know and where do we go from here? Field Crop Res. 132, 95–105.
Klein, I., Gessner, U., Kuenzer, C., 2012. Regional land cover mapping and change detection in Central Asia using MODIS time-series. Appl. Geogr. 35, 219–234.
Kosmas, C., Kirkby, M., Geeson, N., 1999. Manual on Key Indicators of Desertification and Mapping Environmentally Sensitive Areas to Desertification. European Commission (87p).
Kosmas, C., Kairis, O., Karavitis, C., Ritsema, C., Salvati, L., Acikalin, S., et al., 2013. Evaluation and selection of indicators for land degradation and desertification monitoring: methodological approach. Environ. Manag. 54, 951–970.
Kottek, M., Grieser, J., Beck, C., Rudolf, B., Rubel, F., 2006. World map of the Köppen-Geiger climate classification updated. Meteorol. Z. 15, 259–263.
Kraemer, R., Prishchepov, A.V., Müller, D., Kuemmerle, T., Radeloff, V.C., Dara, A., et al., 2015. Long-term agricultural land-cover change and potential for cropland expansion in the former Virgin Lands area of Kazakhstan. Environ. Res. Lett. 10, 054012.
Kundu, A., Dutta, D., 2011. Monitoring desertification risk through climate change and human interference using remote sensing and GIS techniques. Int. J. Geomatics Geosci. 2, 21–33.
Lamchin, M., Lee, J.-Y., Lee, W.-K., Lee, E.J., Kim, M., Lim, C.-H., et al., 2016. Assessment of land cover change and desertification using remote sensing technology in a local region of Mongolia. Adv. Space Res. 57, 64–77.
Li, Z., Chen, Y., Li, W., Deng, H., Fang, G., 2015. Potential impacts of climate change on vegetation dynamics in Central Asia. J. Geophys. Res.-Atmos. 120, 2045–2057.
Li, Q., Zhang, C., Shen, Y., Jia, W., Li, J., 2016. Quantitative assessment of the relative roles of climate change and human activities in desertification processes on the Qinghai-Tibet plateau based on net primary productivity. Catena 147, 789–796.
Lioubimtseva, E., Henebry, G.M., 2009. Climate and environmental change in arid Central Asia: impacts, vulnerability, and adaptations. J. Arid Environ. 73, 963–977.
Loboda, T.V., Giglio, L., Boschetti, L., Justice, C.O., 2012. Regional fire monitoring and characterization using global NASA MODIS fire products in dry lands of Central Asia. Front. Earth Sci. 6, 196–205.
London NSFSD, Unep N, 1994. United Nations Convention to Combat Desertification in Countries Experiencing Serious Drought and/or Desertification, Particularly in Africa.
Ma, Z., Xie, Y., Jiao, J., Li, L., Wang, X., 2011. The construction and application of an Aledo-NDVI based desertification monitoring model. Procedia Environ. Sci. 10, 2029–2035.
Manca, G., Attaway, D.F., Waters, N., 2014. Program assessment and the EU's agrienvironmental measure 214: an investigation of the spatial dynamics of agrienvironmental policies in Sardinia, Italy. Appl. Geogr. 50, 24–30.
Mann, H.B., 1945. Nonparametric tests against trend. Econometrica 13, 245–259.
Mannig, B., Müller, M., Starke, E., Merkenschlager, C., Mao, W., Zhi, X., et al., 2013. Dynamical downscaling of climate change in Central Asia. Global Planet. Change 110, 26–39.
McMillen, D.P., 2004. Geographically Weighted Regression: The Analysis of Spatially Varying Relationships. Oxford University Press.
Mirzabaev, A., Goedecke, J., Dubovyk, O., Djanibekov, U., Le, Q.B., Aw-Hassan, A., 2016. Economics of Land Degradation in Central Asia. Economics of Land Degradation and Improvement–A Global Assessment for Sustainable Development. Springer, pp. 261–290.
Mitchell, T.D., Jones, P.D., 2005. An improved method of constructing a database of monthly climate observations and associated high-resolution grids. Int. J. Climatol. 25, 693–712.
Mohammat, A., Wang, X., Xu, X., Peng, L., Yang, Y., Zhang, X., et al., 2013. Drought and spring cooling induced recent decrease in vegetation growth in Inner Asia. Agric. For. Meteorol. 178-179, 21–30.
Pan, J., Li, T., 2013. Extracting desertification from Landsat TM imagery based on spectral mixture analysis and Albedo-Vegetation feature space. Nat. Hazards 68, 915–927.
Prăvălie, R., Bandoc, G., Patriche, C., Tomescu, M., 2016. Spatio-temporal trends of mean air temperature during 1961–2009 and impacts on crop (maize) yields in the most important agricultural region of Romania. Stoch. Env. Res. Risk A. 31, 1923–1939.
Prăvălie, R., Patriche, C., Bandoc, G., 2017a. Quantification of land degradation sensitivity areas in southern and central southeastern Europe. New results based on improving DISMED methodology with new climate data. Catena 158, 309–320.
Prăvălie, R., Săvulescu, I., Patriche, C., Dumitraşcu, M., Bandoc, G., 2017b. Spatial assessment of land degradation sensitive areas in southwestern Romania using modified MEDALUS method. Catena 153, 114–130.
Prăvălie, R., Piticar, A., Roşca, B., Sfîcă, L., Bandoc, G., Tiscovschi, A., et al., 2019. Spatio-temporal changes of the climatic water balance in Romania as a response to precipitation and reference evapotranspiration trends during 1961–2013. Catena 172, 295–312.
Propastin, P.A., 2008. Inter-annual changes in vegetation activities and their relationship to temperature and precipitation in central Asia from 1982 to 2003. J. Environ. Inf. 12, 75–87.
Robinson, S., 2016a. Land Degradation in Central Asia: Evidence, Perception and Policy. The End of Desertification? Springer, pp. 451–490
Robinson, S., 2016b. Land Degradation in Central Asia: Evidence, Perception and Policy. Springer Berlin Heidelberg.
Safriel, U., Tal, A., 2010. Deserts and desertification: challenges but also opportunities. Land Degrad. Dev. 20, 353–366.
Saiko, T.A., Zonn, I.S., 2000. Irrigation expansion and dynamics of desertification in the Circum-Aral region of Central Asia. Appl. Geogr. 20, 349–367.
Salvati, L., 2012. The spatial nexus between population growth and land degradation in a dry Mediterranean region: a rapidly changing pattern? Chapters 19, 1–8.
Salvati, L., 2014. A socioeconomic profile of vulnerable land to desertification in Italy. Sci. Total Environ. 466–467, 287–299.
Salvati, L., Bajocco, S., 2011. Land sensitivity to desertification across Italy: past, present, and future. Appl. Geogr. 31, 223–231.
Salvati, L., Zitti, M., 2008. Regional convergence of environmental variables: empirical evidences from land degradation. Ecol. Econ. 68, 162–168.
Salvati, L., De Angelis, A., Bajocco, S., Ferrara, A., Barone, P.M., 2013. Desertification risk, long-term land-use changes and environmental resilience: a case study in Basilicata, Italy. Scott. Geogr. J. 129, 85–99.
Salvati, L., Zitti, M., Perini, L., 2016. Fifty years on: long-term patterns of land sensitivity to desertification in Italy. Land Degrad. Dev. 27, 97–107.
Seber, G.A., Lee, A.J., 2012. Linear Regression Analysis. vol. 329. John Wiley & Sons.
Seddon, A.W.R., Maciasfauria, M., Long, P.R., Benz, D., Willis, K.J., 2016. Sensitivity of global terrestrial ecosystems to climate variability. Nature 531, 229.
Sneyers, R., 1991. On the Statistical Analysis of Series of Observations.
Sommer, S., Zucca, C., Grainger, A., Cherlet, M., Zougmore, R., Sokona, Y., et al., 2011. Application of indicator systems for monitoring and assessment of desertification from national to global scales. Land Degrad. Dev. 22, 184–197.
Stulina, G., Eshchanov, O., 2013. Climate change impacts on hydrology and environment in the pre-Aral region. Quat. Int. 311, 87–96.
Su, S., Xiao, R., Li, D., Hu, Y., 2014. Impacts of transportation routes on landscape diversity: a comparison of different route types and their combined effects. Environ. Manag. 53, 636–647.
Tombolini, I., Colantoni, A., Renzi, G., Sateriano, A., Sabbi, A., Morrow, N., et al., 2016. Lost in convergence, found in vulnerability: a spatially-dynamic model for desertification risk assessment in Mediterranean agro-forest districts. Sci. Total Environ. 569-570, 973–981.
UNCCD, 2017. The 13th Meeting of the Parties to the United Nations Convention to Combat Desertification Ordos, China.
Vicente-Serrano, S.M., Schrier, G.V.D., Beguería, S., Azorin-Molina, C., Lopez-Moreno, J.I., 2015. Contribution of precipitation and reference evapotranspiration to drought indices under different climates. J. Hydrol. 526, 42–54.
Vorovencii, I., 2017. Applying the Change Vector Analysis Technique to Assess the Desertification Risk in the South-West of Romania in the Period 1984–2011. Cambridge, UK. 189 p. 524.
Wang, X., Hua, T., Lang, L., Ma, W., 2017. Spatial differences of aeolian desertification responses to climate in arid Asia. Glob. Planet. Chang. 148, 22–28.
Wessels, K.J., van den Bergh, F., Scholes, R.J., 2012. Limits to detectability of land degradation by trend analysis of vegetation index data. Remote Sens. Environ. 125, 10–22.
Xi, X., Sokolik, I.N., 2016. Quantifying the anthropogenic dust emission from agricultural land use and desiccation of the Aral Sea in Central Asia. J. Geophys. Res. Atmos. 121, 270–281.
Yang, L., Wu, J., Shen, P., 2013. Roles of science in institutional changes: the case of desertification control in China. Environ. Sci. Pol. 27, 32–54.
Yu, P.-S., Yang, T.-C., Wu, C.-K., 2002. Impact of climate change on water resources in southern Taiwan. J. Hydrol. 260, 161–175.
Zambon, I., Colantoni, A., Carlucci, M., Morrow, N., Sateriano, A., Salvati, L., 2017. Land quality, sustainable development and environmental degradation in agricultural districts: a computational approach based on entropy indexes. Environ. Impact Assess. Rev. 64, 37–46.
Zhang, C., Lu, D., Chen, X., Zhang, Y., Maisupova, B., Tao, Y., 2016. The spatiotemporal patterns of vegetation coverage and biomass of the temperate deserts in Central

Asia and their relationships with climate controls. Remote Sens. Environ. 175, 271–281.
Zhang, G., Biradar, C.M., Xiao, X., Dong, J., Zhou, Y., Qin, Y., et al., 2017. Exacerbated grassland degradation and desertification in Central Asia during 2000–2014. Ecol. Appl. 28.
Zhao, X., Tan, K., Zhao, S., Fang, J., 2011. Changing climate affects vegetation growth in the arid region of the northwestern China. J. Arid Environ. 75, 946–952.
Zhou, W., Gang, C., Zhou, F., Li, J., Dong, X., Zhao, C., 2015a. Quantitative assessment of the individual contribution of climate and human factors to desertification in northwest China using net primary productivity as an indicator. Ecol. Indic. 48, 560–569.
Zhou, Y., Zhang, L., Fensholt, R., Wang, K., Vitkovskaya, I., Tian, F., 2015b. Climate contributions to vegetation variations in central Asian drylands: pre- and post-USSR collapse. Remote Sens. 7, 2449–2470.